International Journal of Bifurcation and Chaos, Vol. 14, No. 8 (2004) 2875–2884

QUENCHING LORENZIAN CHAOS

RAYMOND HIDE
Department of Mathematics,
Imperial College London, London SW7 2AZ, UK

PATRICK E. McSHARRY
Mathematical Institute, Oxford University,
Oxford OX1 3LB, UK

CHRISTOPHER C. FINLAY* and GUY D. PESKETT
Department of Physics,
Oxford University, Oxford OX1 3PU, UK

Received December 16, 2002

How fluctuations can be eliminated or attenuated is a matter of general interest in the study of steadily-forced dissipative nonlinear dynamical systems. Here, we extend previous work on "nonlinear quenching" [Hide, 1997] by investigating the phenomenon in systems governed by the novel autonomous set of nonlinear ordinary differential equations (ODE's) $\dot{x} = ay - ax$, $\dot{y} = -xzq + bx - y$ and $\dot{z} = xyq - cz$ (where (x, y, z) are time(t)-dependent dimensionless variables and $\dot{x} = dx/dt$, etc.) in representative cases when q, the "quenching function", satisfies $q = 1 - e + ey$ with $0 \leq e \leq 1$. Control parameter space based on a, b and c can be divided into two "regions", an S-region where the persistent solutions that remain after initial transients have died away are steady, and an F-region where persistent solutions fluctuate indefinitely. The "Hopf boundary" between the two regions is located where $b = b_H(a, c; e)$ (say), with the much studied point $(a, b, c) = (10, 28, 8/3)$, where the persistent "Lorenzian" chaos that arises in the case when $e = 0$ was first found lying close to $b = b_H(a, c; 0)$. As e increases from zero the S-region expands in total "volume" at the expense of F-region, which disappears altogether when $e = 1$ leaving persistent solutions that are steady throughout the entire parameter space.

Keywords: Nonlinear quenching; chaos; nonlinear circuits.

1. Introduction

Many investigations of chaos have been concerned with steadily-forced nonlinear dissipative physical systems governed by autonomous sets of nonlinear ODE's in three or more time-dependent variables $\mathbf{x}(t) = (x(t), y(t), z(t), \text{etc.})$, including the celebrated Lorenz [1963] set (see e.g. [Sparrow, 1982; Ott, 1983; Lorenz, 1993; Thompson & Stewart, 2002]). Each set has the general form $\dot{\mathbf{x}}(t) = \mathbf{N}(\mathbf{x}; \mathbf{a})$ if $\dot{\mathbf{x}} = d\mathbf{x}/dt$, where $\mathbf{N}$ includes one or more terms that are nonlinear in the components of $\mathbf{x}$. The non-negative control parameters $\mathbf{a} = (a, b, c, \text{etc.})$ define a "parameter space" which can be divided into two types of region, F and S respectively. An F-region is characterized by solutions exhibiting persistent fluctuations resulting from the instability through Hopf bifurcations of steady equilibrium solutions $\mathbf{x} = \mathbf{x}_0$ satisfying $\dot{\mathbf{x}}_0 = 0$. These solutions are stable within an S-region and therefore persist after initial transients have died away.

*Presently at School of Earth Sciences, University of Leeds, Leeds LS2 9JT, UK.

Of particular interest are forms of $\mathbf{N}$ involving an implicit "quenching function" q that occurs as a factor in mathematical terms representing feedback or coupling, but not in terms representing excitation or damping. Accordingly, the quenching function influences the character of the solutions $\mathbf{x}(t)$ without affecting the equation

$$\frac{d(\mathbf{x}\cdot\mathbf{x})}{dt} = 2\mathbf{x}\cdot\mathbf{N} \tag{1}$$

for overall "energy" balance.

The chosen function q depends in general on one or more of the dependent variables, with certain choices leading to destabilization in the sense that their inclusion expands the F-region at the expense of the S-region. But when studying quenching we are mainly interested in choices that produce the opposite effect, with quenching said to be "complete" if and when the F-region contracts to zero "volume", leaving persistent solutions that are steady throughout the entire parameter space.

The present study was largely prompted by the discovery of examples of complete or partial "nonlinear quenching" with a clear physical origin [Hide, 1997]. The discovery emerged from an investigation of the nonlinear ODE's (see Eqs. (14) and (15) in Sec. 5 below) governing the behavior of certain self-exciting dynamo systems of possible relevance in geophysics, astrophysics and engineering. Guidance provided by Hopf bifurcation analyses in that earlier study was supplemented in subsequent work by analyses of related unforced nondissipative (and therefore conservative) nonlinear systems (see [Hide, 2000] or Eqs. (16) and (17) below). These in turn led to preliminary studies by one of the authors (R. Hide) of quenching in other forced dissipative nonlinear systems, each governed by a set of ODE's formulated by multiplying the feedback or coupling terms of a well-studied set (e.g. Lorenz, Rössler) by various trial quenching functions.

Here, we investigate one of these new sets, namely

$$\dot{x} = ay - ax, \quad \dot{y} = -xzq + bx - y, \quad \dot{z} = xyq - cz \tag{2}$$

where $q = 1 - e + ey$ with $0 \le e \le 1$, in further detail. When $e = 0$ these equations reduce to the Lorenz set, which over extensive regions of parameter space have persistent solutions which fluctuate either periodically or aperiodically (i.e. chaotically). For other values of e it is found that persistent fluctuations are completely quenched when $e = 1$ and partially quenched when $0 < e < 1$.

As expected, q does not appear explicitly in the energy balance equation

$$\frac{d(x^2+y^2+z^2)}{dt} = 2[(a+b)xy - (ax^2 + y^2 + cz^2)] \tag{3}$$

(see (1)), where the first term within the square brackets on the right-hand side represents excitation and the other terms represent damping of various kinds. Significantly, however, q does appear in the corresponding expression for $\operatorname{div}\dot{\mathbf{x}} = \partial\dot{x}/\partial x + \partial\dot{y}/\partial y + \partial\dot{z}/\partial z$, namely

$$\begin{aligned}\operatorname{div}\dot{\mathbf{x}} &= -(a+1+c) - xz\frac{\partial q}{\partial y} \\ &= -(a+1+c) - exz\,. \end{aligned} \tag{4}$$

This scalar is important because it provides insight into the effects of q on the topology of the trajectories of the solutions in (x, y, z) "state" space (see Sec. 3 below).

2. Fixed Point Equilibrium Solutions and Hopf Bifurcations

The coordinates of the fixed points of (2) in state space are the equilibrium solutions (x_0, y_0, z_0) where

$$x_0(\overline{b} - z_0 q_0) = 0, \quad y_0 = x_0, \quad z_0 = \frac{x_0 y_0 q_0}{c}\,, \tag{5}$$

if $q_0 = 1 - e + ey_0$, $(0 \le e \le 1)$ and $\overline{b} = b - 1$. These have a "trivial" solution $(0, 0, 0)$ which is stable or unstable according as $\overline{b} \lessgtr 0$. The two "nontrivial" equilibrium solutions, $\mathbf{x}_0$, that appear when $\overline{b} > 0$ satisfy

$$x_0^2 q_0^2 = c\overline{b}, \quad y_0 = x_0, \quad z_0 = \frac{x_0^2 q_0}{c}\,. \tag{6}$$

Too complicated to write down here are the explicit general expressions for these solutions, which reduce to

$$(x_0,\, y_0,\, z_0) = (\pm(c\overline{b})^{1/2},\, \pm(c\overline{b})^{1/2},\, \overline{b}) \tag{7}$$

when $e = 0$, and to

$$(x_0,\, y_0,\, z_0) = (\pm(c\overline{b})^{1/4},\, \pm(c\overline{b})^{1/4},\, \pm(\overline{b}^3/c)^{1/4}) \tag{8}$$

when $e = 1$.

If small amplitude disturbances about $\mathbf{x}_0$ vary with time as $\exp(nt)$ then the growth rate, n, in

general complex, satisfies a cubic equation of the form

$$n^3 + An^2 + Bn + C = 0\,. \tag{9a}$$

Hopf bifurcations occur when the criteria

$$B > 0 \quad \text{and} \quad AB = C \tag{9b}$$

for the real part of n to change sign can be satisfied by acceptable values of a, b, c and e.

The stability analysis of the general case shows that

$$A = (a + c + 1), \quad B = c(a + b) + (a + 2c)P\,,$$
$$C = 2ac(b - 1 + P)\,, \tag{10a}$$

where

$$P = \frac{4e\overline{b}^{3/2}c^{1/2}}{\{1 - e + [(1 - e)^2 \pm 4e(c\overline{b})^{1/2}]^{1/2}\}^2}\,, \tag{10b}$$

with $P = 0$ when $e = 0$, the Lorenz limit, and $P = \overline{b}$ when $e = 1$. When $0 \le e < 1$ there are acceptable combinations of the control parameters (a, b, c) for which both criteria expressed by (9b) can be satisfied. But the second criterion cannot be satisfied when $e = 1$, implying that the nontrivial fixed points $\mathbf{x}_0$ are then stable for all values of a, b and c.

The second criterion ($AB = C$) leads to an expression for the "Hopf boundary" in an (a, b) régime diagram, upon which $b = b_H$ (say) where $b_H = b_H(a, c; e)$. The expression is complicated in the general case, but when $e = 1$ the boundary disappears (to infinity), and when $e = 0$, the Lorenz limit, b_H is given by simple relationship

$$b_H = \frac{a(a + c + 3)}{a - c - 1}\,. \tag{11}$$

This has acceptable solutions when $a > (c + 1)$ but not when $a \le (c + 1)$. As a increases from $(c + 1)$ — where b_H given by (11) is infinite — b_H decreases at first until it reaches a minimum value at

$$a = a_m = (c + 1) + [2(c + 1)(c + 2)]^{1/2}\,. \tag{12}$$

Thereafter b_H increases monotonically with increasing a and becomes asymptotically equal to a when $a \gg a_m$ (see Fig. 1).

We note here in passing that quenching can occur when q depends linearly on all three dependent variables (cf. (2)), not just y. The nontrivial equilibrium solutions, $\mathbf{x}_0$ still satisfy (6) but the corresponding cubic equation for n is then more complicated than before (cf. (9a) and (10)).

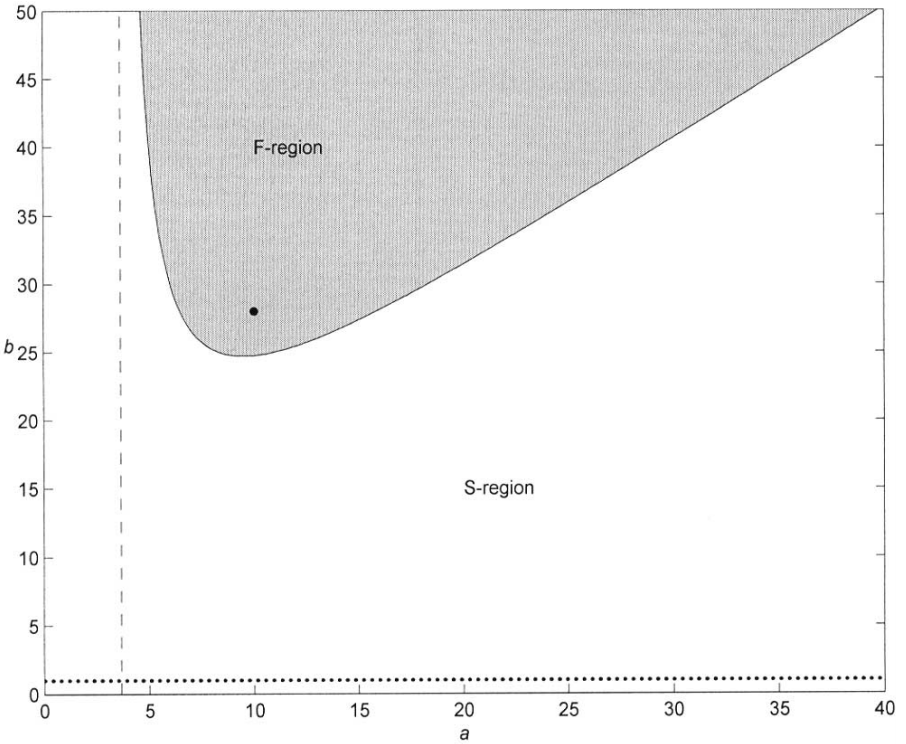

Fig. 1. Hopf boundary $b = b_H(a; c, e)$ in (a, b) space when $e = 0$ and $c = 8/3$, $\{b_H(a; c, 0) = a(a + c + 3)/(a - c - 1)$, see (11)$\}$.

3. Liapunov Exponents

The much-studied point where $(a, b; c) = (10, 28; 8/3)$ [Lorenz, 1963; Sparrow, 1982] lies just above the curve $b = b_H$ given by (11) and close to the minimum at $a = a_m$ (see Fig. 1). For parameter values $a = 10$ and $c = 8/3$, stable fixed points occur within the range $1 < b < 24.74 = b_H$, with transient (i.e. nonpersistent) chaos occurring within the range $13.926 < b < 24.06$. Persistent chaos associated with strange attractors sets in when $b > 24.74$.

One of the hallmarks of chaotic dynamical systems is their sensitive dependence on initial conditions of trajectories in state space, implying that an infinitesimal perturbation is, on average, likely to grow exponentially with time. Such behavior can be quantified by calculating the so-called "Liapunov" exponents $(\Lambda_1, \Lambda_2, \Lambda_3)$, which are real by definition and satisfy $\Lambda_1 \geq \Lambda_2 \geq \Lambda_3$. They provide a measure of local stability for a given trajectory $\mathbf{x}(t)$ [Kantz & Schreiber, 1997], in the absence of which

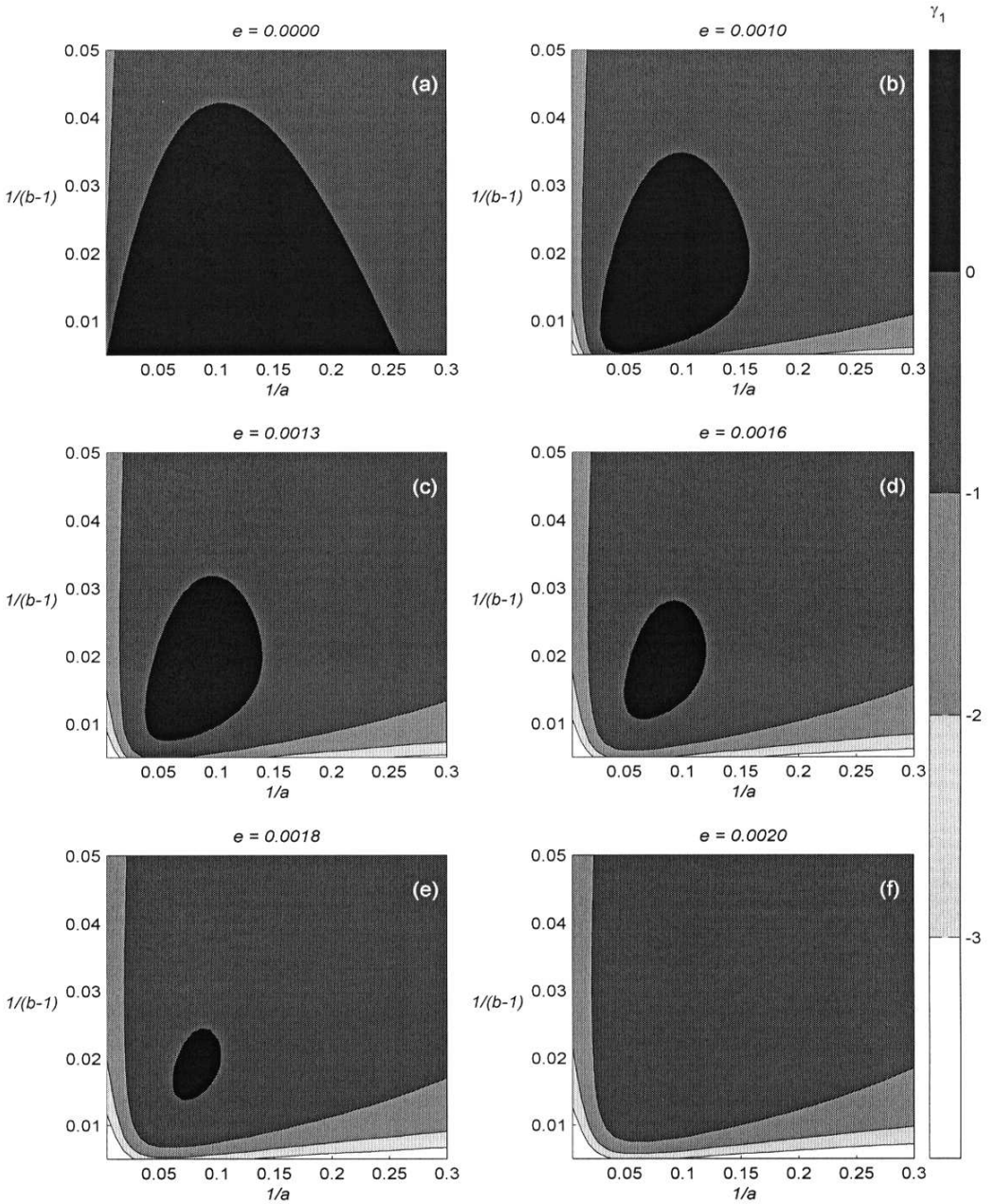

Fig. 2. Hopf bifurcation analyses of (2) showing the largest positive real eigenvalue γ_1 for (a) $e = 0.0000$, (b) $e = 0.0010$, (c) $e = 0.0013$, (d) $e = 0.0016$, (e) $e = 0.0018$, and (f) $e = 0.0020$.

— i.e. when the trajectory reduces to a fixed point — all three exponents are negative. Otherwise their sum is equal to $\operatorname{div} \dot{\mathbf{x}}$ — as given by (4) in the case of (2) — and at least one exponent is equal to zero when the dynamical system is a flow. The system is said to behave chaotically if Λ_1 is positive, implying that near almost every fixed point $\mathbf{x}_0$ there occurs an expansion in at least one direction [Ott *et al.*, 1994]. On the other hand, when $\Lambda_1 = 0$ but $\Lambda_2 < 0$ we have a limit cycle of topological dimension 1, and when $\Lambda_1 = 0$ and $\Lambda_2 = 0$ but $\Lambda_3 < 0$ we have a two-torus attractor of topological dimension 2.

The "tangent propagator" at a fixed point x_0 is given by

$$\mathbf{M}(\mathbf{x}_0, t) = \exp(\mathbf{T}(\mathbf{x}_0, t)), \tag{13}$$

where $\mathbf{T}(\mathbf{x}_0)$ is the Jacobian matrix evaluated at $\mathbf{x}_0$. The largest positive real eigenvalue of $\mathbf{T}(\mathbf{x}_0)$, denoted by γ_1, determines the stability of the system; γ_1 is zero on the Hopf boundary separating parameter space into stable regions (where $\gamma_1 < 0$) and unstable regions (where $\gamma_1 > 0$).

A clearer picture of transitions is provided by régime diagrams with a^{-1} (rather than a) as the abscissa and $(\overline{b}^{-1})$ (rather than b) as the ordinate (where $\overline{b} = b - 1$). Figure 2 gives determinations of Hopf boundaries, where $b = b_H(a, c; e)$, for (2) as obtained from (6), keeping the parameter c fixed at the "Lorenz" value of 8/3.

Computations of corresponding values of γ_1 and Liapunov exponents Λ_1, Λ_2 and Λ_3 were also made (see Figs. 3 and 4), using a numerical procedure described in [Abarbanel *et al.*, 1992]. All exponents are expressed using logarithms to base 2, implying units of "bits per second" (see also [Thompson & Stewart, 2002]). The $\gamma_1 = 0$ contour resulting from the linear analysis of the Lorenz case ($e = 0$) coincides, as expected, with the Hopf boundary, implying no chaotic behavior there. Of course, these results apply only to the positive fixed points given by (7), and with different initial conditions the trajectory may have converged to a chaotic attractor. With this approach, the only way to be absolutely sure that all chaotic behavior has been quenched

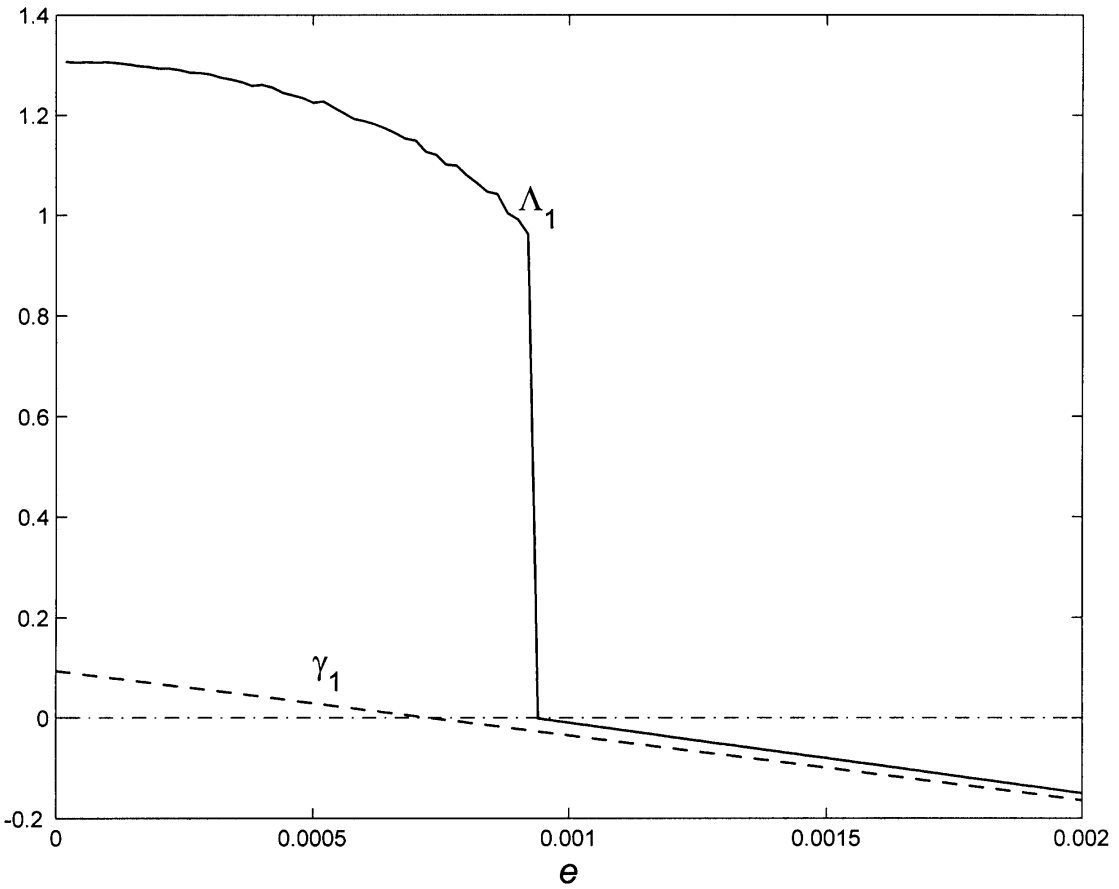

Fig. 3. Variation of γ_1 and Λ_1 with e in solutions of (2) with $a = 10$, $b = 28$ and $c = 8/3$.

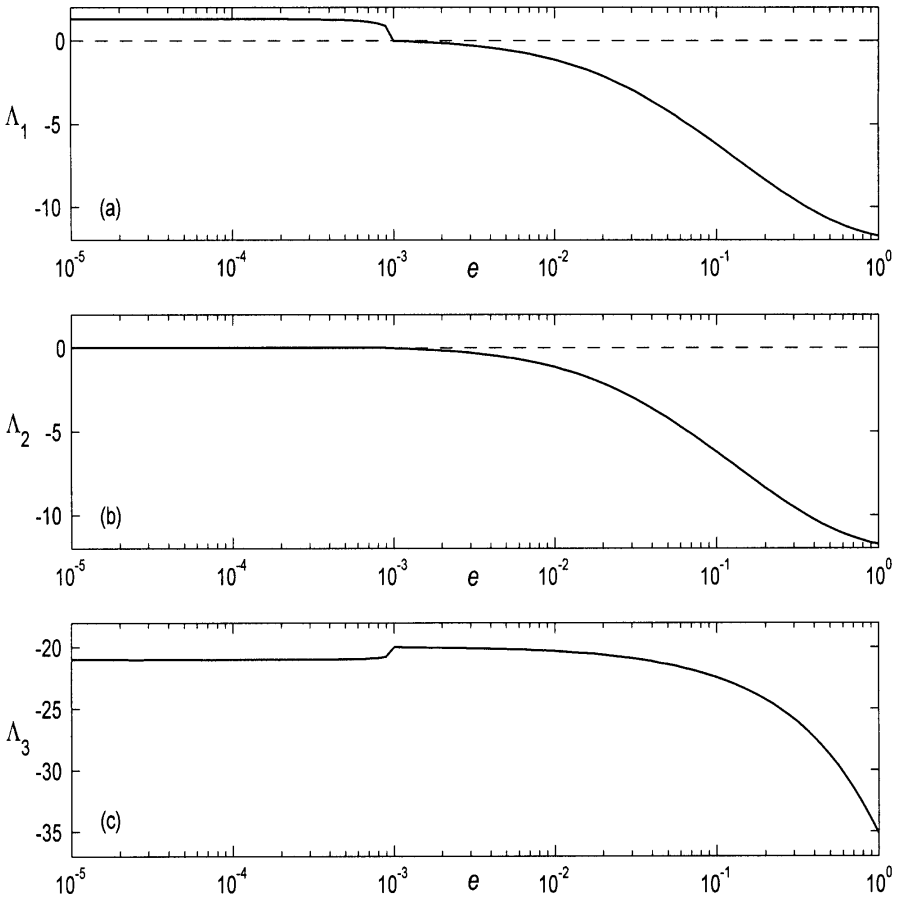

Fig. 4. Liapunov spectra of the solutions of (2) as a function of e when $a = 10$, $b = 28$ and $c = 8/3$.

would be to compute Liapunov exponents for many different initial conditions.

Figure 3 gives the results of comparisons of the first Liapunov exponents, Λ_1 with γ_1 over the range $0 \leq e \leq 0.002$ and for parameter values $(a, b, c) = (10, 28, 8/3)$ (so that $(a^{-1}, \overline{b}^{-1}, c) = (0.1, 0.037, 8/3)$). The value of γ_1 decreases gradually and linearly with increasing e over the whole range covered by e, whereas Λ_1 drops rapidly as it approaches its transition from positive to negative values, and then more slowly and linearly.

Also note that γ_1 is everywhere less than Λ_1, an expected result since γ_1 is based on eigenvalues of $\mathbf{T}(\mathbf{x}_0)$, whereas the Liapunov exponents are based on its singular values. For any asymmetric matrix the eigenvectors are not necessarily equal to the right singular vectors, so that the eigenvalues will systematically underestimate the largest possible growth rate. It is for this reason that perturbations of non-normal systems often exhibit faster growth over small time scales than predicted rates based on stability analyses, which reflect average growth over an infinite span of time [Ziehmann *et al.*, 2000].

4. Analogue Computation of Solutions and Transients

A nonlinear electronic circuit that (ignoring second-order imperfections in its components) had been designed to be governed in its behavior by (2) was used as an accurate and efficient analogue computer for determining the solution trajectories $(x(t), y(t), z(t))$ and investigating their dependence on the control parameters and initial conditions. Details of the circuit used in the present and related work will be described elsewhere. For a detailed review of analogue circuit studies of nonlinear systems see [Luchinsky *et al.*, 1998]. Further details of the measurements presented in this section are given in a dissertation by C. C. Finlay entitled *A Study of Quenching in Two Chaotic Systems* reporting the findings of an M. Phys. project carried out under the supervision of

R. Hide and G. D. Peskett in the Department of Physics at the University of Oxford.

The parameter range accessible in the experiments carried out were $0 \leq a, b, c \leq 100$ and $0 \leq e \leq 1$. The voltage outputs from the circuit were passed to an oscilloscope for displaying and recording not only the time series of each variable but also the phase portraits of any combination of two variables. The figures shown in this section were obtained using the dump facility of the oscilloscope screen.

We chose the parameter values $a = 10$, $b = 50$ and $c = 8/3$ and set the initial conditions to $(x, y, z) = (0, 0, 0)$. In the Lorenz case, $e = 0$, the circuit was able to reproduce the familiar signatures of Lorenzian chaos. In Fig. 5 we display (a) a sample time series for x illustrating aperiodic fluctuations and (b) a phase portrait of $x(t)$ versus $y(t)$ showing Lorenz's famous butterfly.

Having thus tested the circuit successfully against known solutions, we then demonstrated that, in accordance with the findings of Hopf bifurcation analyses given above in Secs. 2 and 3, the chaotic behavior just described could be eliminated by increasing e from 0.0 to 0.1. With this new value of e, the variable x was observed to "quench" at its steady equilibrium value x_0 given by (6), as shown in Fig. 6.

The effect of changing e on the dynamics of the system and phase space topology were investigated by producing time series and phase portraits for values of e equal to 0.000, 0.004, 0.006, 0.010, 0.100 and 1.000, when the system was started at $(x(0), y(0), z(0)) = (0, 0, 0)$ and the subsequent evolution recorded (see Fig. 7). Thus it was found that a tiny change in e was then sufficient to move the system from a fluctuating régime to a steady régime. As e was increased, phase space changed in such a way that trajectories converged more rapidly on stable fixed point solutions given by (6) within the small errors of measurement involved. For larger e the quenched state was

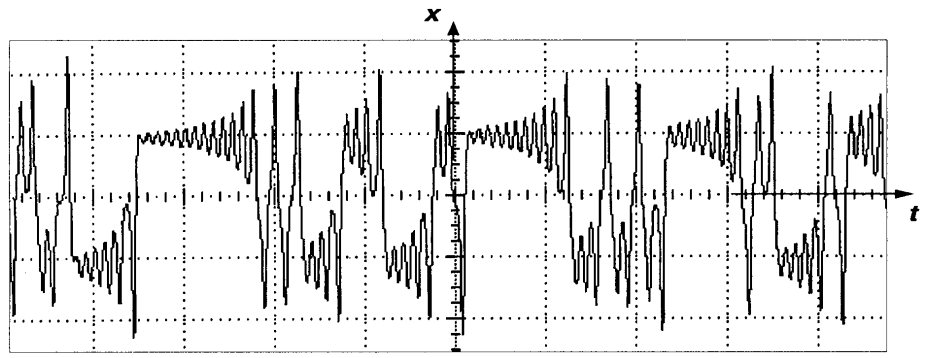

(a)

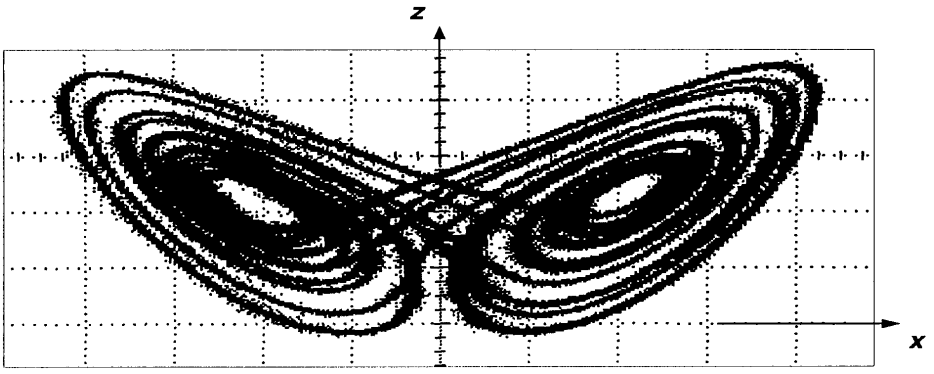

(b)

Fig. 5. Output from a simulation of Lorenz system, when $(a, b, c; e) = (10, 28, 8/3; 0)$. Diagram (a) shows a typical time series of $x(t)$ with aperiodic (i.e. chaotic) fluctuations, and (b) shows a phase portrait of $x(t)$ against $z(t)$ with the solution trajectory following an unpredictable path on a Lorenz strange attractor.

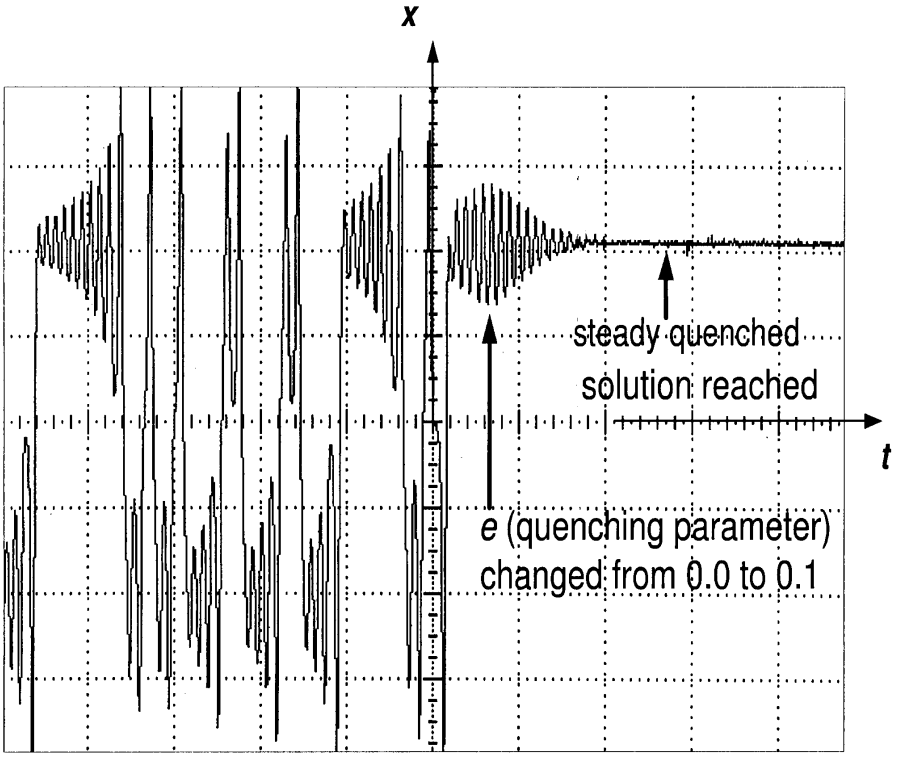

Fig. 6. Observation of nonlinear quenching in the time series of x produced by the electronic circuit simulation. The system is initially in the chaotic fluctuating régime, but when e changes from 0.0 to 0.1 a rapid convergence on one of the predicted quenched solutions is evident.

reached faster and the phase trajectories were less oscillatory.

With c fixed at 8/3 we used the analogue simulation to investigate whether, according to the predictions of Sec. 2, quenching to stable-steady solutions occurred for the whole range of available values of a and b, namely 0 to 100 for each when $e = 1$. Sampling using step sizes of 1.0 for both a and b showed that indeed the solutions that persisted after initial transients had died away were always steady, consistent with the prediction of complete quenching when $e = 1$ (cf. Figs. 1–3 of [Hide, 1997]).

5. Concluding Remarks

Essential in any practical applications of the findings of theoretical studies of quenching will be the ability to interpret the quenching function in clear physical terms. This was possible in the case of the set of nonlinear ODE's in which the quenching phenomenon was first discovered, namely

$$\dot{x} = x(y-1) - \beta z q \qquad \dot{y} = \alpha(1-x^2) - \kappa y\,, \qquad \dot{z} = xq - \chi z\,, \tag{14}$$

where $(\alpha, \beta, \kappa, \chi)$ are positive control parameters [Hide, 1997]. These equations govern the behavior of a steadily-forced single-disk self-exciting dynamo system if x is the dynamo current, y the angular speed of rotation of the disk, z the angular speed of rotation of the armature of the electric motor connected in series with the coil, and xq the torque on the armature of the motor, with

$$q = q(x) = 1 - \overline{e} + \overline{e}x, \quad (0 \le \overline{e} \le 1)\,. \tag{15}$$

Complete quenching was found to occur in this system when $\overline{e} = 1$ and partial quenching when $0 < \overline{e} < 1$ (cf. Sec. 2 above; for further references see [Moroz & Hide, 2000; Moroz, 2002]).

Finally, we note that a common feature of the above-mentioned sets of nonlinear ODE's (namely (2) and (14)) is that when terms representing excitation and damping are excluded, each set reduces to a special case of a much simpler nonlinear set of the form

$$\dot{X} = -YF(X, Y), \quad \dot{Y} = XF(X, Y) \tag{16}$$

(see e.g. [Hide, 2000, Eq. (5.6)]), notably when the arbitrary function $F(X, Y)$ depends linearly on X

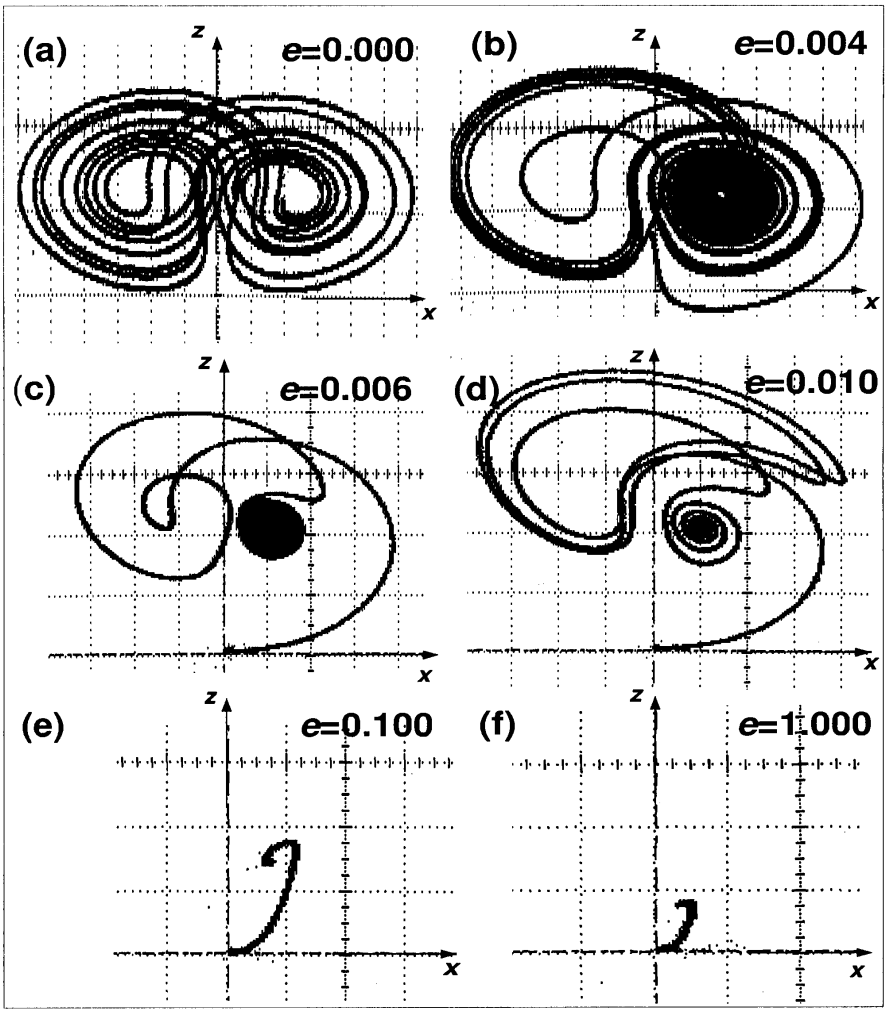

Fig. 7. Phase portraits of $x(t)$ versus $z(t)$ showing the evolution of solution trajectories as e is increased from zero to unity. When $e = 0.000$ the trajectories never settle down, but move on the Lorenz attractor. When a small additional nonlinearity according to the quenching recipe is introduced by increasing e from zero to 0.004, the trajectories spend more time on one side of the attractor than on the other, though over our comparatively short observation time (3000 dimensionless units) no convergence to a steady state was seen. With $e = 0.006$ quenching to a steady state was unambiguously observed, though convergence was very slow. For $e = 0.010$, 0.100 and 1.000, the trajectories home in on quenched solutions with increasing rapidity.

or Y. Equations (16) govern the behavior of a free and undamped nonlinear oscillator and they satisfy

$$X^2 + Y^2 = R^2\,, \tag{17}$$

where R is a constant determined by initial conditions. Thus, irrespective of the form of the function $F(X, Y)$, (16) has solutions with trajectories in the (X, Y) plane lying on a circle of radius R centred at the origin. The speed of angular motion on this circle is equal to $F(X, Y)$, and when R is less than a certain critical value R_c (say), the speed remains nonzero for all values of the polar angle $\tan^{-1}(Y/X)$. Then the system undergoes periodic oscillations, which are nonharmonic except in the special case of harmonic oscillations arising (for all values of R) when F is constant. But when $R > R_c$ oscillations are quenched, there are polar angles where $F(X, Y)$ vanishes, and at least one of which is an "attractor" towards which solutions tend as initial transients die away.

Acknowledgments

R. Hide wishes to thank Professor Vladimir Keilis-Borok and other participants in a discussion meeting on nonlinear processes held in 1998 in Rome for encouraging the present study through their enthusiastic response to the discovery of nonlinear quenching in self-exciting dynamo systems.

References

Abarbanel, H. D. I., Brown, R. & Kennel, M. B. [1992] "Local Liapunov exponents computed from observed data," *J. Nonlin. Sci.* **2**, 343–365.

Hide, R. [1997] "Nonlinear quenching of current fluctuations in a self-exciting homopolar dynamo," *Nonlin. Process. Geophys.* **4**, 201–205.

Hide, R. [2000] "Generic nonlinear processes in self-exciting dynamos and the long-term behaviour of the main geomagnetic field, including polarity superchrons," *Phil. Trans. Roy. Soc. London* **A358**, 943–955.

Kantz, H. & Schreiber, T. [1997] *Nonlinear Time Series Analysis* (Cambridge University Press).

Lorenz, E. N. [1963] "Deterministic nonperiodic flow," *J. Atmos. Sci.* **20**, 130–141.

Lorenz, E. N. [1993] *The Essence of Chaos* (University of Washington Press, Seattle).

Luchinsky, D. G., McClintock, P. V. E. & Dykman, M. I. [1998] "Analogue studies of nonlinear systems," *Repts. Prog. Phys.* **61**, 889–997.

Moroz, I. M. & Hide, R. [2000] "Effects due to induced azimuthal currents in a self-exciting Faraday disk homopolar dynamo with a nonlinear series motor: II. The general case," *Int. J. Bifurcation and Chaos* **10**, 2701–2716.

Moroz, I. M. [2002] "On the behaviour of a self-exciting Faraday disk homopolar dynamo with a variable nonlinear series motor," *Int. J. Bifurcation and Chaos* **12**, 2123–2135.

Ott, E. [1983] *Chaos in Dynamical Systems* (Cambridge University Press).

Ott, E., Sauer, T. & Yorke, J. A. [1994] *Coping with Chaos* (Wiley, NY).

Sparrow, C. [1982] *The Lorenz Equations*: *Bifurcations, Chaos and Strange Attractors* (Springer-Verlag, NY).

Thompson, J. M. T. & Stewart, H. B. [2002] *Nonlinear Dynamics and Chaos*, 2nd edition (Chichester, Wiley).

Ziehmann, C., Smith, L. A. & Kurths, J. [2000] "Localised Liapunov exponents and the prediction of predictability," *Phys. Lett.* **A271**, 237–251.